18

Climatic Response to Anthropogenic Sulfate Forcing Simulated with a General Circulation Model

E. ROECKNER[1], T. SIEBERT[2], and J. FEICHTER[1]
[1]Max-Planck-Institut für Meteorologie, [2]Meteorologisches Institut der Universität Hamburg,
Bundesstraße 55, D–20146 Hamburg, Germany

ABSTRACT

An atmospheric general circulation model coupled to a slab ocean is used to study the climate equilibrium response to changed concentrations of atmospheric CO_2 and anthropogenic sulfate aerosol. It is found that the climate sensitivity of the model does not depend upon the magnitude or character of the forcing but crucially upon its sign. In an experiment, in which both the observed greenhouse forcing over the last 100 years is prescribed (approximately 2 W m^{-2}) and an estimate of the present anthropogenic sulfate burden is calculated by an off-line chemical model, the model predicts a global warming of about 0.5°C, with most of the warming (0.7°C) in the Southern Hemisphere. A net cooling is found over the highly industrialized regions of the Northern Hemsiphere, such as the eastern United States and large parts of Eurasia. In these experiments, a relatively large direct aerosol forcing of globally about 0.7 W m^{-2} is prescribed. On the other hand, indirect aerosol effects through the impact on cloud albedo are not considered, so that the total forcing applied in this study may not be unrealistically large. The results indicate that anthropogenic sulfur emissions in the past should be considered as a potentially important climatic factor.

INTRODUCTION

Since the beginning of industrialization, the levels of atmospheric greenhouse gases such as carbon dioxide (CO_2), methane (CH_4), or nitrous oxide (N_2O) have been increasing due to human activities, e.g., as fossil-fuel combustion, deforestation, and agriculture. Over the last two centuries, fossil-fuel combustion has been the major

Aerosol Forcing of Climate
Edited by R.J. Charlson and J. Heintzenberg

source of the observed 25% increase of atmospheric CO_2 with respect to the preindustrial level. The corresponding global and annual mean radiative forcing of the climate system is about 1.5 W m^{-2} for CO_2 and 1.0 W m^{-2} for the other greenhouse gases (IPCC 1990, Chap. 2). Fossil-fuel combustion is also believed to have a cooling effect on climate through the formation of sulfate aerosols (SO_4) from sulfur dioxide (SO_2) emissions (Wigley 1989; Kaufmann and Fraser 1991; Enghardt and Rodhe 1993). The estimates of the present anthropogenic sulfate forcing range from 0.3 W m^{-2} (Kiehl and Briegleb 1993) to –0.6 W m^{-2} (Charlson et al. 1991) due to the "direct" effect, i.e., the additional backscattering of solar radiation. The "indirect" effect resulting from an increased number concentration of sulfate aerosol particles, more but smaller cloud droplets and, hence, higher cloud albedo (Twomey et al. 1984; Charlson et al. 1987) may even be larger than the direct effect (Charlson et al. 1992). These estimates, however, are much more uncertain than those of the greenhouse-gas forcing because complex physical and chemical processes are involved which are currently not well understood.

The final step, namely, the translation of a radiative forcing into a climatic change is fraught with difficulties as well. Two main problem areas have to be addressed. First, the climatic response does not only depend upon the magnitude and sign of the forcing but also on a variety of poorly understood feedback mechanisms that determine the sensitivity of the climate system to a radiative forcing (IPCC 1990, Chap. 3). Second, the atmosphere does not respond instantaneously to a radiative perturbation. The response time is determined by the slow components of the climate system (ocean and ice).

The appropriate tools for addressing these problems are general circulation models (GCMs) of the atmosphere and ocean (cf. section below on METHODOLOGY). In these models, the climate sensitivity to a prescribed forcing (mostly CO_2 doubling so far) is estimated by means of equilibrium simulations (cf. sections on METHODOLOGY and MODELS). In this chapter, we define global climate sensitivity as the ratio of the global mean surface air temperature change to the global mean radiative forcing at the top of the troposphere. The large variation of the global sensitivity parameter in modern GCMs (0.39–1.23 K/Wm^{-2}) is attributable to the models' varying depiction of cloud feedback processes (Cess et al. 1990).

The other problem area, namely, the delay of the response due to the large thermal inertia of the ocean, is particularly relevant in climate prediction experiments. In these experiments, the evolution of climate change caused by a gradual change of the radiative forcing is the main interest, and the realized climate change, at a given time, will reflect only part of the equilibrium change for the corresponding instantaneous value of the forcing. There is agreement among the scientific community that the response is relatively fast in the tropical oceans, where only a small part of the extra heat is able to penetrate below the thermocline. On the other hand, the response is slow in regions where deep convection plays a role, such as the North Atlantic or the Southern Ocean around Antarctica (Washington and Meehl 1989; Manabe et al. 1991; Cubasch et al. 1992).

Virtually all climate-change experiments performed with GCMs, so far, have been based on greenhouse-gas scenarios, such as an instantaneous doubling or a gradual increase of the atmospheric CO_2 concentration. In this chapter, we analyze the equilibrium response of a GCM to prescribed changes of the atmospheric CO_2 content and the atmospheric sulfate burden that has been estimated from an off-line chemical model. We summarize the basic features of the model and the design of the experiments, present the results, and summarize the major findings.

METHODOLOGY OF CLIMATE CHANGE EXPERIMENTS

The GCMs are based on physical conservation laws which describe the redistribution of mass, momentum, heat, and substances like water vapor in the atmosphere or salinity in the ocean. The governing equations are solved by numerical methods which subdivide the atmosphere (or ocean) vertically into discrete layers wherein the variables are computed. The horizontal variations of each variable are determined either at discrete grid points in finite difference models or by a finite number of prescribed mathematical functions, as in spectral models. The solution of the equations proceeds through time as numerical integration, starting from a specified initial state. The spatial resolution is constrained by the speed and memory of the computer used to perform the simulations. Typical atmospheric models have a horizontal resolution between 300 km and 1000 km and between 10 and 20 levels vertically. Similar resolutions are used in oceanic GCMs. These resolutions only allow the simulation of large-scale features of climate. The fidelity of the GCMs to represent regional details is limited at present.

Because of the coarse resolution, many important processes can be described only in approximate form. These would include the radiative transfer, turbulent and convective transport, and cloud microphysical processes such as condensation, evaporation, and precipitation formation. The model solution requires the specification of upper and lower boundary conditions, for example, the solar constant, orography and land–sea distribution, albedo of bare land, surface roughness, and vegetation characteristics. The coupling of atmospheric and oceanic GCMs is based on the exchange of information at the interface between both models. This information includes state variables, such as sea-surface temperature (SST) or sea-ice amount, but also fluxes of radiation, sensible and latent heat, fresh water (precipitation–evaporation), and momentum.

One of the basic problems that arises through a coupling is the so-called climate drift caused by imperfections of the simulated surface fluxes with the result that the coupled model gradually drifts into an unrealistic climate state. To obtain a realistic unperturbed reference climate for climate-change experiments, flux errors are often neutralized by additive correction terms (flux correction or flux adjustment) derived from uncoupled experiments, in which the surface boundary conditions for the atmosphere and ocean model, respectively, are specified according to observed climatology.

The design of the coupled model as well as the experimental strategy depends upon the problem to be addressed. Due to the large response time of a comprehensive atmosphere–ocean GCM, an equilibrium state (where the global and annual mean absorption of solar radiation is identical to the outgoing longwave radiation at the top of the atmosphere) cannot be achieved with the currently available computer resources. Therefore, in all equilibrium studies, atmospheric GCMs are coupled to dynamically passive ocean models comprising only the upper mixed-layer (typically 50-m thick). To achieve a realistic simulation of the SST, the oceanic heat flux convergence is prescribed appropriately (Hansen et al. 1984). With this simplified model, climate equilibrium is obtained after just a few decades (depending on the magnitude of the forcing and the sensitivity of the model) while thousands of years would be required for a fully coupled GCM. To what extent the results are affected by this simplification is unknown at present. If, on the other hand, the time dependence of the climatic change is the main interest, as in transient-response experiments (IPCC 1990, Chap. 6), a realistic result can only be expected from comprehensive atmosphere–ocean GCMs. Typical simulation times are 100 years (Manabe et al. 1991; Cubasch et al. 1992). In any case, a reference or control experiment without any external perturbation is required, with the climate response then defined as the difference between the perturbed climate state and the control climate. To obtain a reasonably stable estimate of the internal variability in the unperturbed model, a simulation time of several decades is required for the oceanic mixed layer model and several hundred years for the coupled atmosphere–ocean GCM.

MODEL AND EXPERIMENTS

The Model

The atmospheric part of the model used in this investigation is the first-generation model ECHAM1 developed jointly by the Max-Planck-Institute for Meteorology and the University of Hamburg (Roeckner et al. 1992). The dynamics and part of the model physics were adopted from the weather forecast model of the European Centre for Medium-Range Weather Forecasts (ECMWF). Prognostic variables are vorticity, divergence, temperature, (logarithm of) surface pressure, and the mass-mixing ratios of water vapor and cloudwater, respectively. The model equations are solved on 19 vertical levels in a hybrid pressure-sigma system by using the spectral transform method with triangular truncation at wavenumber 21 (T21). Nonlinear terms and physical processes, however, are evaluated at grid-points of a "Gaussian grid" providing a nominal resolution of 5.625° in latitude and longitude. A second-order horizontal diffusion scheme is applied to vorticity, divergence, and temperature. The diffusion is limited, however, to the high wave-number end of the resolved spectrum. The radiation scheme is based on a two-stream approximation of the radiative transfer equations, with six spectral intervals in the terrestrial infrared and four in the solar part of the spectrum. Gaseous absorption due to water vapor, carbon dioxide, and ozone is taken

into account as well as scattering and absorption due to prescribed aerosol- and model-generated clouds. The cloud optical properties are parameterized in terms of the cloudwater content. The cloudwater content is obtained from the respective budget equation, including sources and sinks due to condensation, evaporation, and precipitation formation by coalescence of cloud droplets and sedimentation of ice crystals. Subgrid-scale condensation and cloud formation is taken into account by specifying appropriate thresholds of relative humidity depending on height and convective activity. A Kuo-type convection scheme is employed for penetrative convection, while the effect of shallow convection is parameterized as a diffusion process with appropriate coefficients. The turbulent transfer of momentum, heat, and water vapor is based on the Monin-Obukhov similarity theory for the surface layer and the eddy diffusivity approach above the surface layer. The drag and heat transfer coefficients depend upon roughness length and Richardson number, while the eddy diffusion coefficients depend upon wind shear, mixing length, and Richardson number. The soil model comprises the budgets of heat and water in the soil, the snow pack over land, and the heat budget of permanent land ice. The heat transfer equation is solved in a five-layer model, assuming vanishing heat flux at the bottom. Vegetation effects, such as the interception of rain and snow in the canopy and the stomatal control of evapotranspiration, are parameterized in a highly idealized way. The runoff scheme is based on catchment considerations and takes into account subgrid-scale variations of field capacity over inhomogeneous terrain.

The ocean is represented by a simple slab model with a constant depth of 50 m. The temperature of the slab is calculated from the net heat flux at the surface provided by the atmospheric GCM. To account for model errors as well as for the missing part of the thermodynamic heat budget, such as the oceanic heat transport, an appropriate correction term is calculated from an uncoupled model experiment where the SST is specified according to the observed climatology. This is a standard procedure (Hansen et al. 1984) allowing the model to simulate a realistic control climate. A similar procedure is applied to the thermodynamic sea-ice model, so that the model is able to reproduce realistically the seasonal variation of the sea-ice extent. A realistic simulation of the control climate is crucial, since the response of the climate system depends upon the state of the control climate itself (Hansen et al. 1984; Spelman and Manabe 1984). The model physics remains unaffected by the correction technique. The basic limitation of the model is that the atmosphere–ocean coupling is confined to the exchange of heat. Any feedbacks that might result from a change of the ocean circulation in a changing climate cannot be considered.

Sensitivity Experiments

Apart from a control experiment of the present-day climate, three experiments have been performed with different radiative perturbations. In the first experiment, the atmospheric CO_2 concentration is doubled with respect to the present value, as in many other GCMs before (IPCC 1990, Chap. 3, Table 3.2a). In the second experiment, the

radiative forcing due to present-day anthropogenic sulfate aerosol burden is prescribed. The anthropogenic sulfate burden is obtained from simulations of the global sulfur cycle with and without anthropogenic sulfur sources, respectively (Langner and Rodhe 1991), and the direct radiative forcing is mimicked by a change of the surface albedo ΔR_s according to the algorithm developed by Charlson et al. (1991):

$$\Delta R_s = \beta\delta \sec\Phi_o \, (1 - R_s)^2 \,, \tag{18.1}$$

where the aerosol optical thickness δ is the product of the aerosol burden $B(SO_4^{2-})$ and the mass scattering coefficient $R = 8.5\ m^2 g^{-1}$, as in the study by Charlson et al. (1991). β is the backscattered fraction (0.29) of the scattered flux, Θ_o the solar zenith angle and R_s the surface albedo. In this experiment, an annual mean value of $B(SO_4^{2-})$ is prescribed. Nevertheless, the radiative forcing has a strong seasonal component due to the seasonal variation of the solar irradiance. It is important to note that the sign of the forcing is positive in this experiment, i.e., the surface albedo is decreased with respect to the control experiment. The reason for this assumption is that the anthropogenic sulfate cooling is implicitly included already in the present-day control climate. Hence, in this experiment, a preindustrial climate is simulated without anthropogenic sulfur but with the present level of atmospheric CO_2.

Finally, in the last experiment, both the greenhouse warming and the sulfate cooling are considered together. Starting from the present-day control climate, the CO_2 content is increased instantaneously by 40% and the surface albedo is increased according to the algorithm 18.1 in contrast to the second experiment, where the surface albedo is decreased. The CO_2 increase is consistent with the total anthropogenic greenhouse-gas forcing of approximately 2 W m^{-2} estimated for the last 100 years (IPCC 1990, Chap. 2), and the surface albedo change is considered as the radiative impact of the present anthropogenic sulfate in the atmosphere according to the model simulation of Langner and Rodhe (1991). Hence, in the third experiment, the radiative forcing is an estimate of the anthropogenic contribution to the total radiative forcing which may have influenced our climate during the last 100 years. It is important to note, however, that the simulated reference state refers to the present climate. A list of the experiments is shown in Table 18.1.

Table 18.1 List of experiments.

Exp. No.	Notation	Change of atmospheric concentration	Simulation time (years)	Averaging period (years)
	Control		25	last 20
1	CO_2	Doubling of current concentration (345 ppmv)	45	last 20
2	SO_4	Anthropogenic SO_4 *removal*	45	last 20
3	$CO_2 + SO_4$	CO_2 + 40% and *addition* of anthropogenic SO_4	45	last 20

RESULTS

The global and annual mean radiative forcings and the respective changes of surface air temperature are shown in Table 18.2 together with the climate sensitivity parameter, defined as the ratio of the global mean temperature response and the global mean radiative forcing at the top of the troposphere (Cess et al. 1990). The global mean sulfate forcing of –0.7 W m^{-2} in experiment 2 is slightly larger than the –0.6 W m^{-2} estimated by Charlson et al. (1991) based on a similar input (Langner and Rodhe 1991). There are two reasons for this discrepancy. First, our estimate is based on a more recent simulation of the sulfur cycle (J. Langner, pers. comm.) with better estimates of the anthropogenic emissions, including biomass burning and industrial emissions in the Southern Hemisphere (Chile and South Africa). Second, the radiative forcing of the climate system depends not only upon the radiative change in the aerosol layer but also on the transmissivity of the atmosphere and on cloud cover, which is not prescribed according to observations, as in the study of Charlson et al., but simulated by the model.

The temperature change in the 2 × CO_2 experiment of 2.8°C is on the lower side of the changes simulated by GCMs so far (1.9°C–5.2°C; see IPCC 1990, Chap. 3, Table 3.2a). It is interesting to note that the sensitivity in the sulfate experiment 2 is identical to that in the CO_2 experiment 1. A preliminary conclusion would be that the climate sensitivity does not depend upon the magnitude and character of the forcing. In the CO_2 experiment, forcing is mainly in the longwave part of the spectrum, while in the sulfate experiment only the solar radiation is affected. There is also a difference in the regional distribution of the forcing. Due to the relatively short mean residence time of atmospheric sulfur, the anthropogenic sulfate forcing is concentrated over the main industrial emission regions (Figure 18.1). The CO_2 forcing, on the other hand, is more widespread, and spatial inhomogeneities are related to gradients of atmospheric state variables, such as temperature, water vapor, and clouds, rather than to the distribution of industrial emissions (Kiehl and Briegleb 1993). The apparent independence of global climate sensitivity on the distribution of the radiative forcing has been discussed in detail by Hansen et al. (1984), who showed that the climatic response caused by CO_2 doubling is virtually identical to that caused by a 2% increase of the solar constant.

Table 18.2 Global and annual averages of the top-of-troposphere radiative forcing, surface air temperature change, and global sensitivity parameter as analyzed from the experiments.

Exp. No.	Radiative forcing (W m^{-2})	Change of surface air temperature (K)	Climate sensitivity parameter (K/W m^{-2})
1	4.0	2.8	0.7
2	0.7	0.5	0.7
3	1.3	0.5	0.4

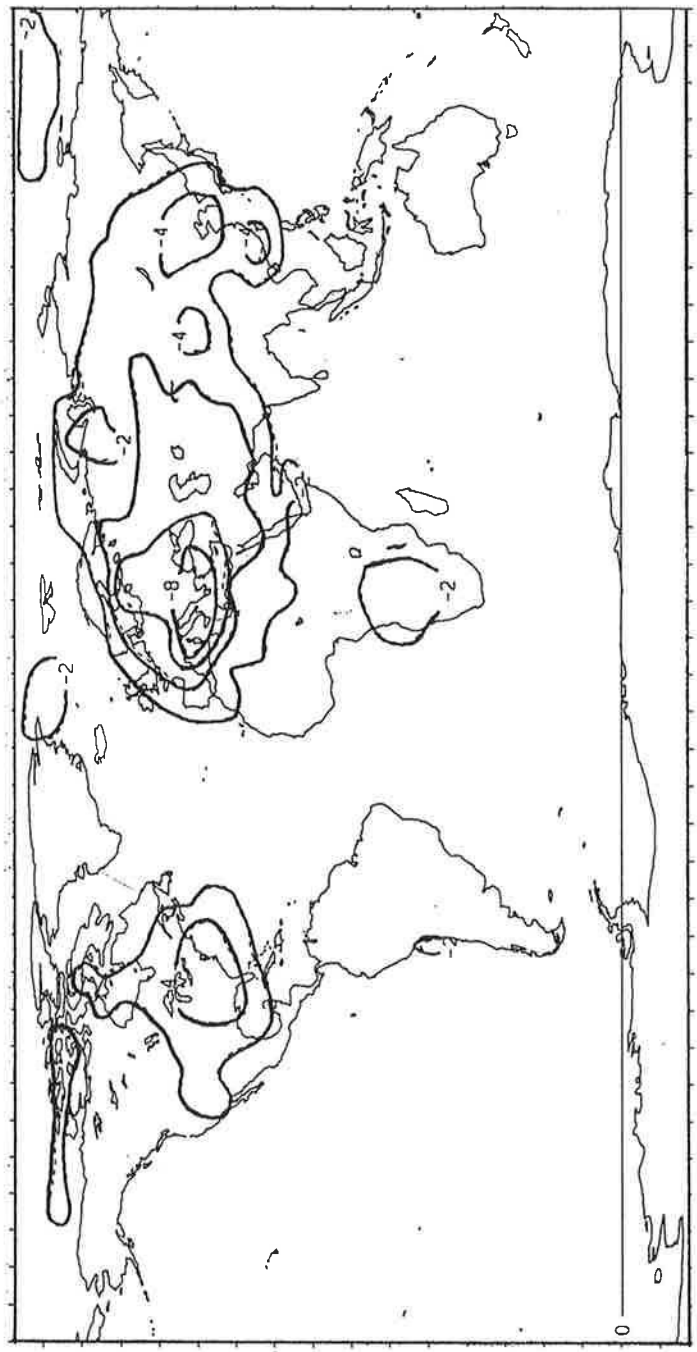

Figure 18.1 Radiative forcing (W m^{-2}) at the top of the atmosphere for the month of July.

In experiment 3, however, where both greenhouse warming and sulfate cooling is considered, the sensitivity is significantly smaller than in experiments 1 and 2, where only a positive forcing is prescribed. One possible explanation for the reduced sensitivity is that the relatively large sulfate forcing over the continents in the Northern Hemisphere offsets the greenhouse forcing in these areas so that important positive feedback mechanisms, such as the ice/snow-albedo-temperature feedback, cannot be activitated in the Northern Hemisphere. Moreover, the strength of the ice-albedo feedback seems to depend upon the sign of the forcing, as suggested by Spelman and Manabe (1984) and Manabe et al. (1991), who explained the substantially larger climate sensitivity for CO_2 halving (cooling!), as compared to CO_2 doubling, with the progression of the ice and snow lines towards lower latitudes with larger solar irradiance where the ice/snow-albedo feedback becomes increasingly important.

The geographical distribution of the annual mean temperature changes is shown in Figure 18.2. For the sake of comparison, in Figure 18.2a the $2 \times CO_2$ response is scaled according to the greenhouse forcing of 2 W m^{-2} used in the ($CO_2 + SO_4$) experiment (Figure 18.2c). The implied assumption of linearity between the forcing and the response may be justified by the relatively small amount of the forcing. Figure 18.2b shows the annual mean temperature difference between the control climate and experiment 2, in which the radiative impact of the anthropogenic sulfate burden is removed.

The CO_2 response in Figure 18.2a shows many features familiar from previous equilibrium studies (IPCC 1990, Chap. 5), such as the poleward amplification of the surface warming by the ice-albedo feedback and the land–sea contrast with higher temperatures over the continents in general. In the sulfate experiment (Figure 18.2b), the marked hemispheric asymmetry of the response is related to the larger radiative forcing in the Northern Hemisphere (Figure 18.1). Although the response is relatively large over the main industrial regions, such as the U.S., Europe, and East Asia, there is also a large remote component with a pronounced cooling over the Arctic and a peculiar warming pattern over northeastern Canada. The wave train over North America is caused by a shift in the position of the stationary waves which, in the control experiment, have larger amplitudes than in the real atmosphere (Roeckner et al. 1992).

A comparison of Figure 18.2a (experiment 1) and Figure 18.2c (experiment 3) suggests that sulfate cooling may offset much of the greenhouse warming in the Northern Hemisphere with a net cooling over major parts of Eurasia and over the eastern part of the U.S. As in the sulfate experiment 2, the strong remote response over northeastern Canada and parts of Greenland may be an artifact of this particular model. In the Southern Hemisphere, the greenhouse warming is clearly larger than the sulfate cooling. The hemispheric means are 0.3°C and 0.7°C for the Northern and Southern Hemispheres, respectively.

Although the simulated global annual mean equilibrium warming of about 0.5°C is within the range of the warming observed during the past 100 years (0.3° to 0.6°C; IPCC 1990), it should be noted that the simulated warming refers to a hypothetical equilibrium state, while the observed realized warming is a result of the transient

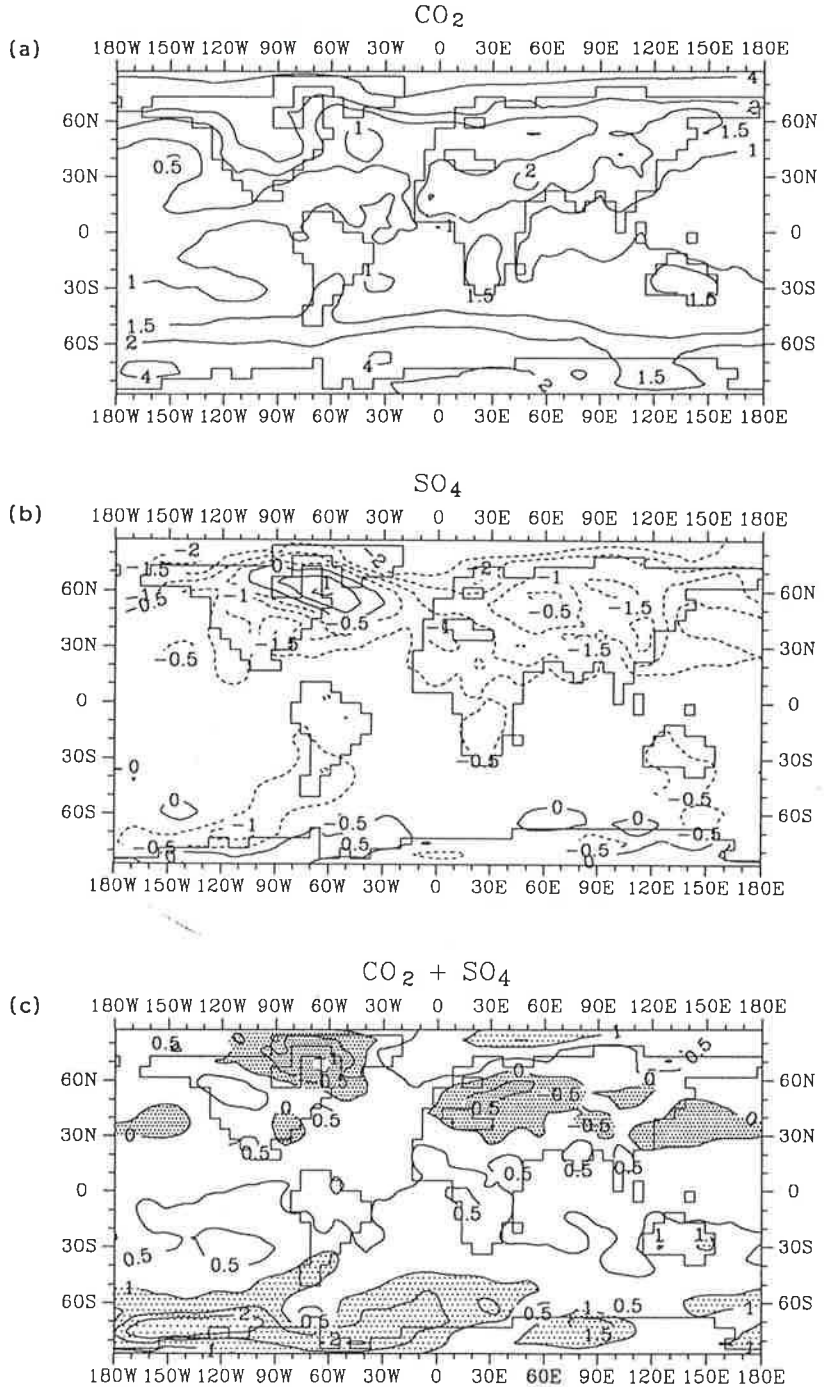
(a)
CO2
180W 150W 120W 90W 60W 30W 0 30E 60E 90E 120E 150E 180E
60N
30N
0
30S
60S
(b)
SO4
(c)
CO2 + SO4

response of the whole climate system to a time-dependent forcing superimposed by natural variability at various time scales.

Consistent with the asymmetric temperature response in the polar regions, with hardly any warming in the Arctic but substantial warming around Antarctica (Figure 18.2c), the Arctic sea-ice area remains virtually unchanged in the (CO_2 + SO_4) experiment (cf. the full and dotted curves in Figure 18.3c), while the area covered with sea ice around Antarctica is reduced by roughly 10% (cf. the dashed curves in Figure 18.3c). In the CO_2-doubling experiment, on the other hand (Figure 18.3a), the Arctic sea-ice loses 30% of its area as compared to the control experiment (ctrl), and the Antarctic sea-ice loses about 50%. The changes of the mean sea-ice volume, however, are significant even in the (CO_2 + SO_4) experiment with losses of about 5% in the Arctic and 25% around Antarctica (not shown).

SUMMARY AND DISCUSSION

The equilibrium response studies, which addressed the relative role of past CO_2 and SO_2 emissions, indicate that both may have influenced our climate over the past 100 years. According to these simulations, the anthropogenic greenhouse effect is dominant in the Southern Hemisphere, where the model predicts an equilibrium warming of about 0.7°C, while in the Northern Hemisphere the sulfate cooling largely offsets the greenhouse warming so that the total warming is less than 0.3°C. A net cooling is simulated over industrialized regions, e.g., the U.S., Europe, and East Asia. The relatively large remote response over parts of Canada and Greenland may be an artifact of the model, which tends to overestimate the amplitude of the stationary waves.

A striking aspect of the simulations is that the model sensitivity seems to be independent of the magnitude and character of the forcing but highly dependent upon its sign. Sensitivity is relatively large if the sign is negative, while it is considerably smaller if the sign is positive. The process that seems to determine this asymmetry is the snow/ice-albedo feedback, which becomes increasingly important if the climate starts to cool. These results are consistent with those of Manabe et al. (1991), who obtained a significantly larger sensitivity in a CO_2-halving (climate cooling) experiment than in a CO_2-doubling experiment.

Figure 18.2 (a) Annual mean surface air temperature change (°C) where 50% of the 2 × CO_2 response is shown, equivalent to a forcing of approximately 2 W m^{-2} at the top of the tropopause. (b) The temperature difference (°C) between the control experiment and an experiment is shown where the SO_4 is removed from the present climate. Negative values are stippled. (c) Annual mean temperature change (°C) with respect to the present for the combined (CO_2 + SO_4) forcing during the last 100 years. Dark shading denotes cooling and light shading warming of more than 1 K.

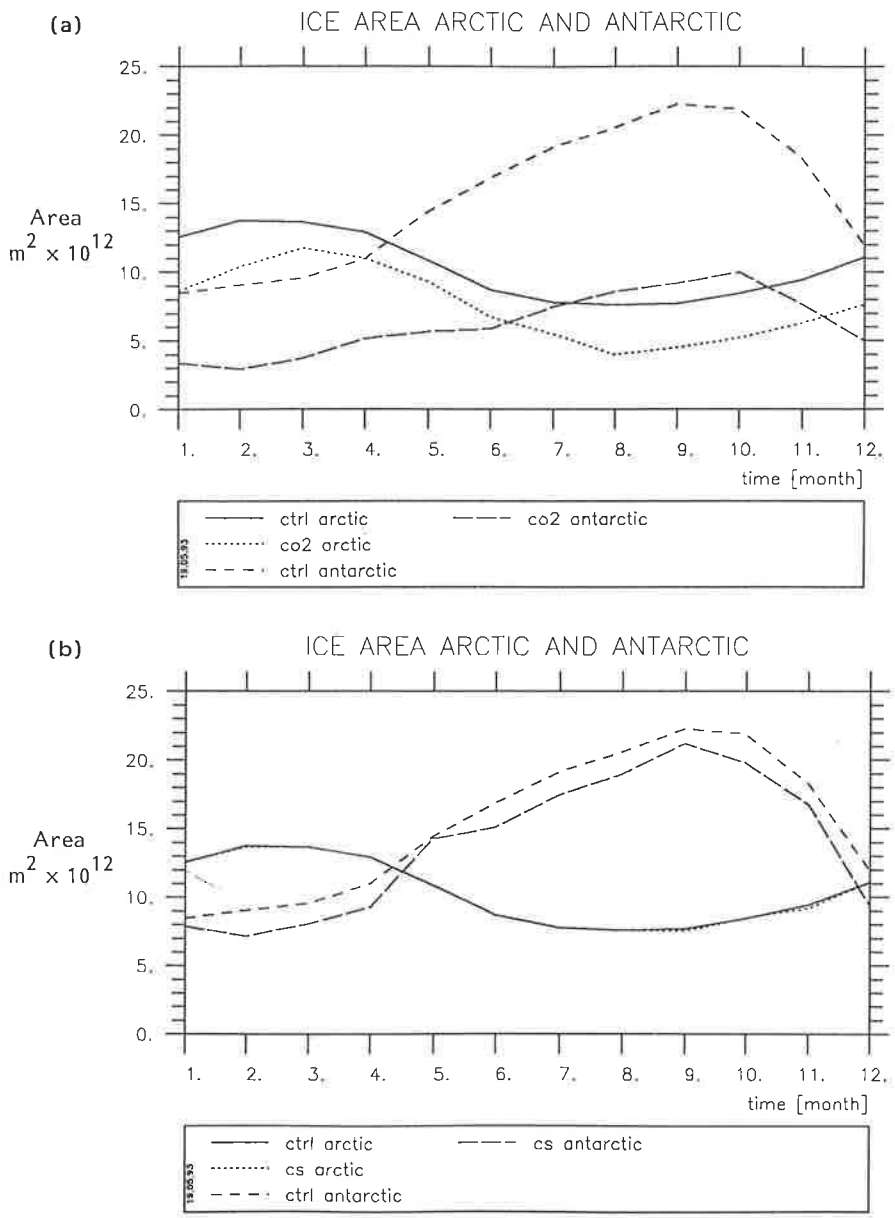

Figure 18.3 Seasonal cycle of the Arctic and Antarctic sea-ice areas. (a) Control experiment together with the 2 x CO_2 experiment (1), denoted by "co2." (b) Control experiment together with the (CO_2 + SO_4) experiment (3), denoted by "cs."

The regionally confined forcing resulting from anthropogenic sulfur emissions is reflected in the climate response; however, remote effects are evident as well, particularly in the Arctic. The poleward amplification of the warming, which is a characteristic feature of CO_2-forcing experiments but without observational evidence so far, is significantly reduced in the Southern Hemisphere and totally offset in the Northern Hemisphere if a modest sulfate aerosol forcing (35%) is added to the greenhouse forcing. Consequently, the sea-ice area in the Arctic remains practically unchanged and the mean sea-ice thickness is only slightly reduced.

Changes of climate-state variables, such as cloudiness, precipitation, or wind, appear to be insignificant. Likewise, changes of the diurnal temperature range, which might be expected as a result of enhanced backscattering of solar radiation in areas of strong aerosol forcing, are related to the spatially incoherent changes of cloudiness rather than to the aerosol forcing patterns.

Although the direct aerosol effect is possibly overestimated in this study (Kiehl and Briegleb 1993), the indirect effect is not considered, so that the total aerosol forcing of about 0.7 W m^{-2} prescribed in the experiment may not be excessively high.

A similar investigation has been performed recently by Taylor and Penner (1994), who coupled the NCAR Community Climate Model CCM1 with the Lawrence Livermore National Laboratory tropospheric chemistry model. Although the sensitivity of the CCM1 is significantly larger than that of ECHAM1, and the details of the remote response are different, the overall structure of the response is similar to that shown in this study. In both studies, the climate equilibrium response has been calculated with a simple oceanic mixed-layer model, so that a comparison with the observational record of this century is problematic. Future work should address the indirect aerosol effect as well as the coupling of the atmospheric GCM with the deep ocean for transient response studies, so that a comparison with observed data would be more meaningful.

ACKNOWLEDGMENTS

This work was sponsored by the Bundesminister für Forschung und Technologie, Grant 07 KFT 535 to the University of Hamburg, and by the Commission of the European Community, contract number PL 910 385 to the Max-Planck-Institute of Meteorology. We thank Henning Rodhe and Joakim Langner for providing us with the sulfate data.

REFERENCES

Cess, R.D., G.L. Potter, J.P. Blanchet, G.J. Boer, A.D. Del Genio, M. Déqué, V. Dymnikov, V. Galin, W.L. Gates, S.J. Ghan, J.T. Kiehl, A.A. Lacis, H. Le Treut, Z.-X. Li, X.-Z. Liang, B.J. McAvaney, V.P. Meleshko, J.F.B. Mitchell, J.-J. Morcrette, D.A. Randall, L. Rikus, E.

Roeckner, J.F. Royer, U. Schlese, D.A. Sheinin, A. Slingo, A.P. Sokolow, K.E. Taylor, W.M. Washington, R.T. Wetherald, I. Yanai, and M.-H. Zhang. 1990. Intercomparison and interpretation of climate feedback processes in 19 atmospheric general circulation models. *J. Geophys. Res.* **95:**16,601–16,615.

Charlson, R.J., J. Langner, H. Rodhe, and S.G. Warren. 1991. Perturbation of the northern hemisphere radiative balance by backscattering from anthropogenic sulfate aerosols. *Tellus* **43AB:**152–163.

Charlson, R.J., J.E. Lovelock, M.O. Andreae, and S.G. Warren. 1987. Oceanic phytoplankton, atmospheric sulphur, cloud albedo and climate. *Nature* **326:**655–661.

Charlson, R.J., S.E. Schwartz, J.M. Hales, R.D. Cess, J.A. Coakley, Jr., J.E. Hansen, and D.J. Hofmann. 1992. Climate forcing by anthropogenic aerosols. *Science* **255:**423–430.

Cubasch, U., K. Hasselmann, H. Höck, E. Maier-Reimer, U. Mikolajewicz, B.D. Santer, and R. Sausen. 1992. Time-dependent greenhouse warming computations with a coupled ocean–atmosphere model. *Clim. Dyn.* **8:**55–69.

Engardt, M., and H. Rodhe. 1993. A comparison between patterns of temperature trends and sulfate aerosol pollution. *Geophys. Res. Lett.* **20:**117–120.

Hansen, J., A. Lacis, D. Rind, G. Russel, P. Stone, I. Fung, R. Ruedy, and J. Lerner. 1984. Climate sensitivity: Analysis of feedback mechanisms. In: Climate Processes and Climate Sensitivity, ed. J.E. Hansen and T. Takahashi, pp. 130–163. Maurice Ewing Series 5. Washington, D.C.: American Geophysical Union.

IPCC (Intergovernmental Panel on Climate Change). 1990. Climate Change. The IPCC Scientific Assessment, ed. J.T. Houghton, G.J. Jenkins, and J.J. Ephraums. Cambridge: Cambridge Univ. Press, 365 pp.

Kaufman, Y.J., and R.S. Fraser. 1991. Fossil fuel and biomass burning effect on climate—Heating or cooling? *J. Clim.* **4:**578–588.

Kiehl, J.T., and B.P. Briegleb. 1993. The relative roles of sulfate aerosols and greenhouse gases in climate forcing. *Science* **260:**311–314.

Langner, J., and H. Rodhe. 1991. A global three-dimensional model of the tropospheric sulfur cycle. *J. Atmos. Chem.* **13:**225–263.

Manabe, S., R.J. Stouffer, M.J. Spelman, and K. Bryan. 1991. Transient responses of a coupled ocean–atmosphere model to gradual changes of atmospheric CO_2. I. Annual mean response. *J. Clim.* **4:**785–818.

Roeckner, E., K. Arpe, L. Bengtsson, S. Brinkop, L. Dümenil, M. Esch, E. Kirk, F. Lunkeit, M. Ponater, B. Rockel, R. Sausen, U. Schlese, S. Schubert, and M. Windelband. 1992. Simulation of the present-day climate with the ECHAM model: Impact of model physics and resolution. Report No. 93. Hamburg: Max-Planck-Institut für Meteorologie, 171 pp.

Spelman, M.J., and S. Manabe. 1984. Influence of oceanic heat transport upon the sensitivity of a model climate. *J. Geophys. Res.* **89:**571–586.

Taylor, K.E., and J.E. Penner. 1994. Climate system response to aerosols and greenhouse gases: A model study. *Nature* **369:**734–737.

Twomey, S.A., M. Piepgrass, and T.L. Wolfe. 1984. An assessment of the impact of pollution on global cloud albedo. *Tellus* **36B:**356–366.

Washington, W.M., and G.A. Meehl. 1989. Climate sensitivity due to increased CO_2: Experiments with a coupled atmosphere and ocean general circulation model. *Clim. Dyn.* **4:**1–38.

Wigley, T.M.L. 1989. Possible climate change due to SO_2 derived cloud condensation nuclei. *Nature* **339:365–367.**